

# Pion mass dependence of the nucleon mass and chiral extrapolation of lattice data in the chiral quark soliton model

K. Goeke,<sup>1</sup> J. Ossmann,<sup>1</sup> P. Schweitzer,<sup>1</sup> and A. Silva<sup>2</sup>

<sup>1</sup>*Institut für Theoretische Physik II, Ruhr-Universität Bochum, D-44789 Bochum, Germany*

<sup>2</sup>*Departamento de Física and Centro de Física Computacional, Universidade de Coimbra, P-3000 Coimbra, Portugal*  
(Dated: March, 2005)

The dependence of the nucleon mass on the mass of the pion is studied in the framework of the chiral quark-soliton model. A remarkable agreement is observed with lattice data from recent full dynamical simulations. The possibility and limitations to use the results from the chiral quark soliton model as a guideline for the chiral extrapolation of lattice data are discussed. A comparison to other extrapolation approaches based on chiral perturbation theory and the finite range regulator method is made.

PACS numbers: 13.60.Hb, 12.38.Lg, 12.39.Ki, 14.20.Dh

## I. INTRODUCTION

The formulation of QCD on a discrete, finite Euclidean lattice [1] is at present the only strict and model independent approach allowing to solve QCD in the low energy regime and to study, e.g., the hadronic spectrum from first principles [2]. Numerical lattice QCD simulations face technical problems, such as discretization errors or finite size effects, which are attacked and minimized with increasing success by employing improved versions of discretized actions, or by working on larger lattices available thanks to the steadily growing computer power. Still, present lattices are too small to accommodate the pion as light as it appears in nature [3–10].

The tool needed to extrapolate lattice data from the region of nowadays typically  $m_\pi \gtrsim 400$  MeV down to the physical value of the pion mass is, in principle, provided by the chiral perturbation theory ( $\chi$ PT). The  $\chi$ PT is an effective but rigorous approach to the description of low energy phenomena of strong interactions [11, 12]. It is based on the concept of spontaneous chiral symmetry breaking with the pion as the Goldstone boson which acquires a small mass only due to explicit chiral symmetry breaking by the small current masses of the light quarks. In  $\chi$ PT it is not possible to compute baryon masses, which serve to absorb counter-terms necessary to regularize chiral loops and must be renormalized anew in each order of the chiral expansion. However,  $\chi$ PT allows to address such questions like, e.g., how much do baryon masses change if one “switches” on the masses of light quarks and varies their values.

In order to extrapolate reliably lattice data by means of  $\chi$ PT it is important to ensure the convergence of the chiral expansion up to large values of  $m_\pi$ . A first and promising *matching* of  $\chi$ PT and lattice results was reported, and it was established that the chiral expansion is well under control up to  $m_\pi^2 < 0.4$  GeV<sup>2</sup> [13–15], see also [7]. More conservative estimates, however, indicate that the chiral expansion is reliable only up to  $m_\pi^2 < 0.1$  GeV<sup>2</sup> [16]. In this situation it is desirable to have a description and control of an intermediate region of pion masses, which would go beyond a matching and certify a safe *overlap* between the regime of the validity of  $\chi$ PT and the lattice data. Here studies in chiral models may provide helpful insights.

In Refs. [17–21] the concept was introduced and de-

veloped to regularize chiral loops by means of suitable vertex form factors, referred to as “finite range regulators” and intended to simulate physical effects of the pion cloud which has a finite range due to  $m_\pi \neq 0$ . In a certain sense the finite range regulator method corresponds to a chiral resummation reliable up to  $m_\pi^2 < 1$  GeV<sup>2</sup> as argued in [21]. While being physically intuitive and appealing, the approach was criticized to be unsatisfactory from a field-theoretic point of view, since it gives preference of one (“finite range”) regularization scheme to another (e.g. “dimensional”) regularization scheme [13].

In this work we present a study of the (implicit) pion mass dependence of the nucleon mass in the chiral quark soliton model ( $\chi$ QSM) [22, 23]. This model was derived under certain assumptions from the instanton model of the QCD vacuum [24, 25], which provides a dynamical picture of the chiral symmetry breaking mechanism [26]. In this model the nucleon appears as a soliton of the chiral pion mean field in the limit of a large number of colours  $N_c$ . The model provides a theoretically consistent description of numerous baryonic quantities ranging from static properties [27, 28] over “usual” [29] till “generalized” parton distribution functions [30], which – as far as these quantities are known – agrees with phenomenology to within (10 – 30)%.

The  $\chi$ QSM incorporates the correct leading non-analytic terms [31] in the large  $N_c$  limit which, however, does not commute with the chiral limit [11, 32, 33]. We will show that the model correctly describes also the heavy quark limit. All this makes the  $\chi$ QSM a suitable and appealing ground for the study we have in mind.

In fact, we will show that the  $\chi$ QSM provides a satisfactory description of the *variation* of the nucleon mass  $M_N$  with  $m_\pi$  up to  $m_\pi = 1.5$  GeV. We shall discuss that the results from the  $\chi$ QSM offer a guideline how to extrapolate lattice data. We shall, however, also comment on the limitations of this approach which lie in the nature of the non-commutativity of the large- $N_c$  limit and the chiral limit.

This note is organized as follows. In Sect. II the effective theory, on which the  $\chi$ QSM is founded, is briefly introduced. In Sect. III the model results are compared to lattice QCD results. In Sect. IV a comparison is made to  $\chi$ PT and the finite range regulator (FRR) approach. Sect. V contains the conclusions. App. A contains technical details on regularization, and App. B gives a digression on the pion-nucleon sigma-term.

## II. PION AND NUCLEON IN THE EFFECTIVE THEORY

Let us consider the effective theory which was derived from the instanton model of the QCD vacuum [24, 25] and is given by the partition function [34, 35]

$$Z_{\text{eff}} = \int \mathcal{D}\psi \mathcal{D}\bar{\psi} \mathcal{D}U \exp \left( i \int d^4x \bar{\psi} (i\partial - MU\gamma^5 - m)\psi \right), \quad (1)$$

where  $U = \exp(i\tau^a \pi^a)$  denotes the  $SU(2)$  chiral pion field with  $U\gamma^5 = \exp(i\gamma_5 \tau^a \pi^a)$ , and  $M$  is the dynamical (“constituent”) quark mass due to spontaneous breakdown of chiral symmetry, and  $m = m_u = m_d$  is the current quark mass. We neglect throughout isospin breaking effects.

The effective theory (1) is valid at low energies below a scale set by the inverse of the average instanton size  $\rho_{\text{av}}^{-1} \approx 600$  MeV. The dynamical mass is momentum dependent, i.e.  $M = M(p)$ , and goes to zero for  $p \gg \rho_{\text{av}}^{-1}$ . In practical calculations it is convenient to replace  $M(p)$  by a constant mass  $M$ , and to regularize the effective theory within an appropriate regularization scheme with a cut-off of  $\mathcal{O}(\rho_{\text{av}}^{-1})$ . In the present work we use  $M = 350$  MeV based on the instanton vacuum model [26].

In the effective theory (1) chiral symmetry is spontaneously broken and a non-zero quark-vacuum condensate  $\langle \bar{\psi}\psi \rangle \equiv \langle \text{vac} | (\bar{\psi}_u \psi_u + \bar{\psi}_d \psi_d) | \text{vac} \rangle$  appears which is given in leading order of the large- $N_c$  limit by the quadratically UV-divergent Euclidean loop integral

$$\langle \bar{\psi}\psi \rangle = - \int \frac{d^4 p_E}{(2\pi)^4} \frac{8N_c M'}{p_E^2 + M'^2} \Big|_{\text{reg}} = -8N_c M' I_1(m), \quad (2)$$

where  $I_1$  is its proper-time regularized version, see App. A, and  $M' \equiv M + m$ . Note that in QCD strictly speaking  $\langle \bar{\psi}\psi \rangle$  is well-defined only in the chiral limit. The pion is not a dynamical degree of freedom in the theory (1). Instead the dynamics of the pion field appears only after integrating out the quark fields which yields the effective action

$$S_{\text{eff}}[U] = \frac{f_\pi^2}{4} \int d^4x \text{tr} \partial^\mu U \partial_\mu U^\dagger + \dots \quad (3)$$

where the dots denote the four-derivative Gasser-Leutwyler terms with correct coefficients, the Wess-Zumino term, terms  $\propto m$  (and an infinite series of higher-derivative terms) [23]. The pion decay constant  $f_\pi = 93$  MeV in Eq. (3) is given in the effective theory by the logarithmically UV-divergent loop integral (whose regularized version we denote by  $I_2$ , see App. A)

$$f_\pi^2 = \int \frac{d^4 p_E}{(2\pi)^4} \frac{4N_c M'^2}{(p_E^2 + M'^2)^2} \Big|_{\text{reg}} = 8N_c M'^2 I_2(m). \quad (4)$$

The mass of the pion can be determined from the position of the pole of the pion propagator in the effective theory (1). Its relation to the current quark mass is given by the equation

$$m_\pi^2 = \frac{m}{M} \frac{I_1(m)}{I_2(m)}, \quad (5)$$

which, for small current quark masses  $m$ , corresponds to the Gell-Mann–Oakes–Renner relation

$$m_\pi^2 f_\pi^2 = -m \langle \bar{\psi}\psi \rangle + \mathcal{O}(m^2). \quad (6)$$

The  $\chi$ QSM is an application of the effective theory (1) to the description of baryons [22, 23]. The large- $N_c$  limit allows to solve the path integral over pion field configurations in Eq. (1) in the saddle-point approximation. In the leading order of the large- $N_c$  limit the pion field is static, and one can determine the spectrum of the one-particle Hamiltonian of the effective theory (1)

$$\hat{H}|n\rangle = E_n|n\rangle, \quad \hat{H} = -i\gamma^0 \gamma^k \partial_k + \gamma^0 M U \gamma^5 + \gamma^0 m. \quad (7)$$

The spectrum consists of an upper and a lower Dirac continuum, distorted by the pion field as compared to continua of the free Dirac-Hamiltonian

$$\hat{H}_0|n_0\rangle = E_{n_0}|n_0\rangle, \quad \hat{H}_0 = -i\gamma^0 \gamma^k \partial_k + \gamma^0 M + \gamma^0 m, \quad (8)$$

and of a discrete bound state level of energy  $E_{\text{lev}}$ , if the pion field is strong enough. By occupying the discrete level and the states of the lower continuum each by  $N_c$  quarks in an anti-symmetric colour state, one obtains a state with unity baryon number. The soliton energy  $E_{\text{sol}}$  is a functional of the pion field

$$E_{\text{sol}}[U] = N_c \left[ E_{\text{lev}} + \sum_{E_n < 0} (E_n - E_{n_0}) \right]_{\text{reg}}. \quad (9)$$

$E_{\text{sol}}[U]$  is logarithmically divergent, see App. A for the explicit expression in the proper-time regularization. By minimizing  $E_{\text{sol}}[U]$  one obtains the self-consistent solitonic pion field  $U_c$ . This procedure is performed for symmetry reasons in the so-called hedgehog ansatz

$$\pi^a(\mathbf{x}) = e_r^a P(r), \quad U(\mathbf{x}) = \cos P(r) + i\tau^a e_r^a \sin P(r), \quad (10)$$

with the radial (soliton profile) function  $P(r)$  and  $r = |\mathbf{x}|$ ,  $\mathbf{e}_r = \mathbf{x}/r$ . The nucleon mass  $M_N$  is given by  $E_{\text{sol}}[U_c]$ . The self-consistent profile satisfies  $P_c(0) = -\pi$  and decays in the chiral limit as  $1/r^2$  at large  $r$ . For finite  $m$  it exhibits a Yukawa tail  $\propto \exp(-m_\pi r)/r$  with the pion mass  $m_\pi$  connected to  $m$  by the relation (5).

For the following discussion we note that the soliton energy can be rewritten as an expansion in powers of  $\partial^\mu U$  as follows

$$E_{\text{sol}}[U] = \sum_{k=1}^{\infty} F_k [(\partial U)^k] \quad (11)$$

where  $F_k [(\partial U)^k]$  symbolically denotes a functional in which  $\partial^\mu U$  appears  $k$ -times (appropriately contracted). Note that in leading order of the large- $N_c$  limit the soliton field is time-independent, i.e.  $\partial U$  is just  $\nabla U$ . For some observables the lowest orders in expansions analog to (11) were computed [27–30].

Let us also remark that in the case  $m_u = m_d = m_s$  the above given formulae for the soliton energy in the  $SU(2)$  version of the model coincide with those from the  $SU(3)$  version [28].

In order to describe properties of the nucleon other than the mass, it is necessary to integrate over the zero modes of the soliton solution in the path integral, which assigns a definite momentum, and spin and isospin quantum numbers to the baryon. Corrections in the  $1/N_c$ -expansion can be included by considering time dependent pion field fluctuations around the solitonic solution. The  $\chi$ QSM allows to evaluate baryon matrix elements

of local and non-local QCD quark bilinear operators like  $\langle B' | \bar{\Psi} \Gamma \Psi | B \rangle$  (with  $\Gamma$  denoting some Dirac- and flavour-matrix) with no adjustable parameters, which explains the wide range of applicability of this model [27–30].

### A. The mass of the nucleon in the large- $N_c$ limit

If one managed to solve QCD in the limit  $N_c \rightarrow \infty$  one would in principle obtain for the mass of the nucleon an expression of the form (let the  $M_i$  be independent of  $N_c$ )

$$M_N = N_c M_1 + N_c^0 M_2 + N_c^{-1} M_3 + \dots \quad (12)$$

The  $\chi$ QSM provides a practical realization of the large- $N_c$  picture of the nucleon [36], and respects the general large- $N_c$  counting rules. In leading order of the large- $N_c$  limit one approximates in the  $\chi$ QSM the nucleon mass by the expression for the soliton energy in Eq. (9), i.e. one considers only the first term in the expansion (12)  $M_N \approx N_c M_1 = E_{sol}$ . We obtain numerically<sup>1</sup>

$$M_N = 1254 \text{ MeV} \quad (13)$$

where the cutoff in the regulator function  $R$ , see App. A, is chosen such that for  $m_\pi = 140 \text{ MeV}$  the physical value of the pion decay constant  $f_\pi$  is reproduced. We observe an overestimate of the physical value  $M_N = 940 \text{ MeV}$  by about 30%. This is not surprising, given the fact that we truncate the series in Eq. (12) after the first term and thus neglect corrections which are generically of  $\mathcal{O}(1/N_c)$ , i.e. of the order of magnitude of the observed overestimate.

In fact, the soliton approach is known to overestimate systematically the physical values of the baryon masses because of – among others – spurious contributions due to the soliton center of mass motion [37]. Taking into account the corresponding corrections, which are  $\mathcal{O}(N_c^0)$ , reduces the soliton energy by the right amount of about 300 MeV. (Note that there are also other sources of corrections at  $\mathcal{O}(N_c^0)$ , see Ref. [37].) We shall keep in mind this systematic overestimate, when we will discuss lattice data below.

### B. The chiral limit

In the following we will be interested in particular in the pion mass dependence of the nucleon mass. From  $\chi$ PT we know that

$$M_N(m_\pi) = M_N(0) + A m_\pi^2 + B m_\pi^3 + \dots \quad (14)$$

where the dots denote terms which vanish faster than  $m_\pi^3$  with  $m_\pi \rightarrow 0$ . The constants  $M_N(0)$  and  $A$  (which is related to the pion-nucleon sigma-term) serve to absorb infinite counter-terms in the process of renormalization in  $\chi$ PT – in the sense of renormalizability in  $\chi$ PT. However,

the constant  $B$ , which accompanies the so-called leading non-analytic (in  $m$ , since  $m_\pi^3 \propto m^{3/2}$ ) contribution, is finite. For this constant  $\chi$ PT, as well as any theory which correctly incorporates chiral symmetry, yields [11, 32]

$$B = k \frac{3g_A^2}{32\pi f_\pi^2} \quad (15)$$

with  $k = 1$  for finite  $N_c$ . However, the limits  $m_\pi \rightarrow 0$  and  $N_c \rightarrow \infty$  do not commute. If we choose first to take  $N_c \rightarrow \infty$  while keeping  $m_\pi$  finite, and only then we consider the chiral limit, then  $k = 3$ . The reason for that is the special role played by the  $\Delta$ -resonance. In the large- $N_c$  limit the nucleon and the  $\Delta$ -resonance become mass-degenerated<sup>2</sup>

$$M_\Delta - M_N = \mathcal{O}(N_c^{-1}) \quad (16)$$

Taking  $N_c \rightarrow \infty$  while  $m_\pi$  is kept finite, one has  $M_\Delta - M_N \ll m_\pi$  and has to consider the contribution of the  $\Delta$ -resonance as intermediate state in chiral loops on equal footing with the contribution of the nucleon. The contribution of the  $\Delta$ -resonance appears (in quantities which do not involve polarization) to be twice the contribution of the nucleon, hence  $k = 3$  [33]. This is the situation in the  $\chi$ QSM and, in fact, in this model one recovers [31] the correct (in the large- $N_c$  limit) leading non-analytic term in Eq. (15).

### C. The heavy quark limit

The  $\chi$ QSM is based on chiral symmetry which consideration makes sense only when explicit chiral symmetry breaking effects are small. Nevertheless one can consider the model, in principle, for any value of  $m$ . In this context let us first note that taking the limit of large current quark masses in Eqs. (2, 4, 5) yields

$$\lim_{\text{large } m} m_\pi = 2m \quad (17)$$

which is the correct heavy quark limit for the mass of a meson (see Sec.II D on details of parameter fixing). As a remnant of the original Goldstone boson character of the pion the limit in Eq. (17) is approached from above, see Table 1. This is in contrast to other mesons or baryons for which the *reduction* of the mass due to binding forces becomes more and more negligible in the heavy quark (i.e. non-relativistic) limit.

What happens to the mass of the soliton in this limit? Consider the eigenvalue problem in Eq. (7). With increasing  $m$  the “potential term”  $MU^{75}$  is less and less important and the spectrum of the full Hamiltonian (7) becomes more and more similar to the spectrum of the free Hamiltonian (8). In this limit the eigenvalues of the

<sup>1</sup> In this work we quote numerical results to within an accuracy of 1 MeV. However, one should keep in mind that we neglect isospin breaking effects (and electromagnetic corrections). Therefore we shall round off the physical masses as  $m_\pi = 140 \text{ MeV}$  and  $M_N = 940 \text{ MeV}$ , and the same is understood for our numerical results.

<sup>2</sup> Though in the  $\chi$ QSM one cannot handle  $\mathcal{O}(N_c^0)$  corrections to  $M_N$ , still one is able to describe consistently the mass difference ( $M_\Delta - M_N$ ) and to reproduce the large- $N_c$  counting rule in Eq. (16) by considering a class of particular (so-called “rotational”)  $1/N_c$ -corrections [25]. In the soliton picture  $\Delta$  and nucleon are just different rotational states of the same classical soliton. In this note we do not consider rotational corrections and work to leading-order in the large- $N_c$  expansion.

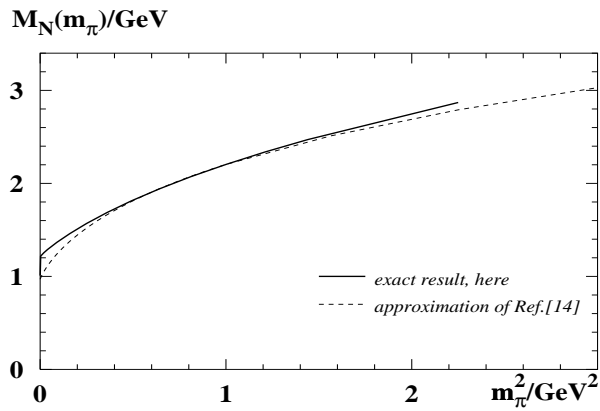


FIG. 1: Nucleon mass  $M_N(m_\pi)$  vs.  $m_\pi^2$  in the chiral quark-soliton model. Solid line: Exact result obtained here. Dashed line: The approximation based on the instanton vacuum model from Ref. [31].

full and free Hamiltonian nearly cancel in the sum over energies in Eq. (9). Only the contribution of the discrete level is not compensated and approaches  $E_{\text{lev}} \approx m \rightarrow \infty$ . Thus, we recover the correct heavy quark limit

$$\lim_{\text{large } m} M_N = N_c m. \quad (18)$$

However, the above considerations are formal, since the crucial step consists in demonstrating that a stable soliton solution indeed exists, i.e. that a self-consistent profile can be found for which the soliton energy (9) takes a minimum. In practice, we find that stable soliton solutions exist at least up to  $m = \mathcal{O}(700 \text{ MeV})$ , which is sufficient for a comparison to lattice QCD results. In this range we observe a tendency to approach the limit (18) from below as expected, see Table I. Thus, we find that both the pion and the nucleon mass are correctly described in the effective theory when the current mass of the quarks becomes large.

#### D. Fixing of parameters

When studying the nucleon mass as function of  $m_\pi$  we must specify what is fixed and what varies in the chiral limit. Here we keep the dynamical constituent quark mass  $M = 350 \text{ MeV}$  fixed, and choose to keep  $f_\pi = 93 \text{ MeV}$  fixed. The latter is a choice which is often considered in literature (though strictly speaking  $f_\pi$  does also vary with  $m_\pi$ ). This means that the precise value of the cutoff  $\Lambda_{\text{cut}} = \mathcal{O}(\rho_{\text{av}}^{-1})$  in the proper time regularization scheme must be adjusted anew for a given  $m_\pi$ , see Table I. Whether other choices, e.g., allowing  $f_\pi$  to be  $m_\pi$ -dependent, also yield consistent descriptions is subject of current investigations.

In the above-described way we obtain the results shown in Table I.  $M_N(m_\pi)$  from the  $\chi$ QSM is plotted as solid line in Fig. 1. The meaning of the dashed curve in Fig. 1 is explained in App. B where a digression is given on the pion-nucleon sigma-term related to the slope of  $M_N(m_\pi)$ .

TABLE I: The dependence on the pion mass for fixed  $f_\pi = 93 \text{ MeV}$  in the  $\chi$ QSM. All numbers are in units of MeV. Rows 2,3,4: Current quark mass  $m$ , cutoff of the effective theory  $\Lambda_{\text{cut}}$ , and quark vacuum condensate  $\langle \bar{\psi}\psi \rangle$  depend on  $m_\pi$  according to Eqs. (2, 4, 5).  $\Lambda_{\text{cut}}$  is of the order of magnitude of the inverse of the average instanton size  $\rho_{\text{av}}^{-1} \approx 600 \text{ MeV}$ . Note that in QCD – in contrast to effective theories with a well defined regularization prescription – the notion of quark vacuum condensate for  $m \neq 0$  is ambiguous. Rows 5,6,7: Contributions of the discrete level  $N_c E_{\text{lev}}$  and the continuum  $N_c E_{\text{cont}}$  to the total soliton energy  $E_{\text{sol}} = N_c(E_{\text{lev}} + E_{\text{cont}})$ , see Eq. (9), to be identified with the nucleon mass in the model. The numerical numbers confirm within the studied range of  $m$  the heavy quark limit discussed in Sec. II C.

$m_\pi$	$m$	$\Lambda_{\text{cut}}$	$\langle \bar{\psi}\psi \rangle^{1/3}$	$N_c E_{\text{lev}}$	$N_c E_{\text{cont}}$	$E_{\text{sol}}$
0	0	649	-350	681	530	1211
10	0.1	649	-350	682	530	1212
50	2	648	-345	692	526	1218
140	16	643	-328	744	510	1254
300	69	635	-281	872	494	1366
600	223	666	-210	1202	484	1686
1200	556	799	-137	2006	465	2471

### III. COMPARISON TO LATTICE DATA

In this Section we compare  $M_N(m_\pi)$  from  $\chi$ QSM with lattice results on the nucleon mass from Refs. [4–10]. Wherever possible we will use only such lattice data, where all bare lattice parameters were kept fixed apart from the current quark mass (or the hopping parameter).

$M_N(m_\pi)$  from the model overestimates the lattice data by about 300 MeV which is expected, if we recall the discussion in Sec. II A. Remarkably we observe that it is possible to introduce an  $m_\pi$ -independent subtraction constant  $C = \mathcal{O}(300 \text{ MeV})$  depending on the lattice data, such that  $[M_N(m_\pi) - C]$  agrees well with the lattice data.

In Fig. 2a we compare the  $\chi$ QSM result for  $M_N(m_\pi)$  to full lattice data by the UKQCD and QCDSF Collaborations [6, 7] obtained from simulations on  $(16 - 24)^3 \times 48$  lattices using the standard Wilson plaquette action for gauge fields and the non-perturbatively  $\mathcal{O}(a)$  improved action for fermions. The fat points in Fig. 2a were extracted from simulations at  $5.20 \leq \beta \leq 5.29$  on lattices of the physical size  $L \geq 1.96 \text{ fm}$  with  $m_\pi L > 6$  and lattice spacings  $a = 0.09 \text{ fm}$  to  $0.12 \text{ fm}$  fixed by the Sommer method with  $r_0 = 0.5 \text{ fm}$  [38]. Other lattice spacings quoted below were also determined by means of this popular method which, however, is not free of criticism [39]. A best fit yields  $C = 329 \text{ MeV}$  with a  $\chi^2$  per degree of freedom of  $\chi_{\text{dof}}^2 = 0.7$  and is shown in Fig. 2a. The uncertainty of the constant  $C$  due to the statistical error of the lattice data is of the order of magnitude of few MeV and thus negligible, see the remarks in footnote 1.

For comparison in Fig. 2a also data by the UKQCD and QCDSF Collaborations [6, 7] are shown from smaller lattices  $L = 1.5 \text{ fm}$  to  $1.7 \text{ fm}$ . Finite size effects are clearly visible, and were subject to a detailed study in Ref. [7]. Since the present  $\chi$ QSM calculation by no means is able to simulate finite volume effects, we restrict our study to data from lattices with  $L \gtrsim 2 \text{ fm}$ . The study of Ref. [7] indicates that for lattices of this size finite volume ef-

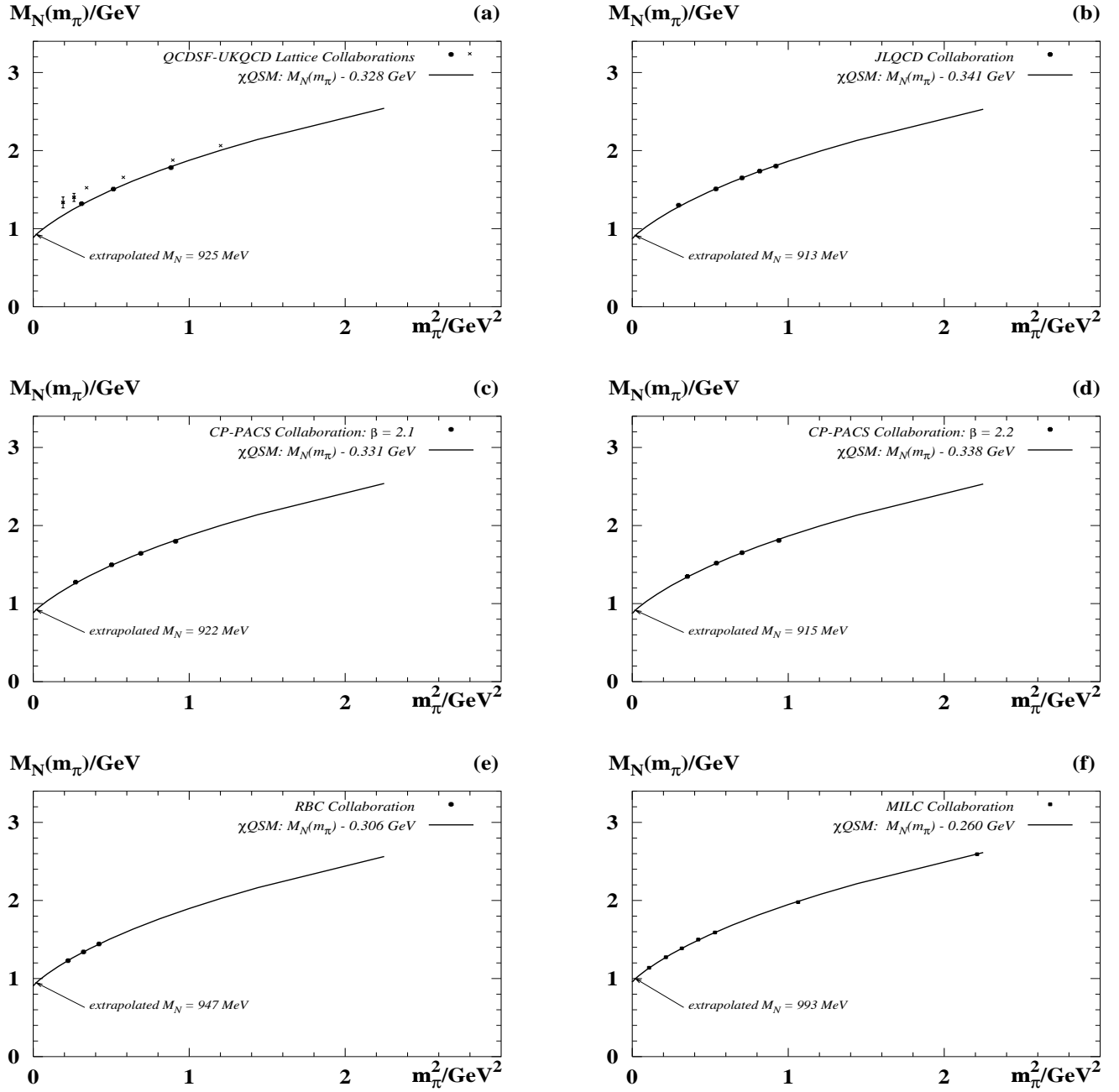


FIG. 2:  $M_N(m_\pi)$  vs.  $m_\pi^2$  from the chiral quark-soliton model vs. lattice data on  $M_N(m_\pi)$  from full simulations by (2a) the UKQCD-QCDSF Collaborations [6, 7], (2b) the JLQCD Collaboration [5], (2c,d) the CP-PACS Collaboration [4], (2e) the RBC Collaboration [8], (2f) the MILC Collaboration [9]. All data were obtained from large lattices  $L \gtrsim 2$  fm, with the exception of the data marked by crosses in (2a), see text. Unless error bars are shown, here and in the following figures the statistical error of the lattice data is comparable to or smaller than the size of the points in the plot.

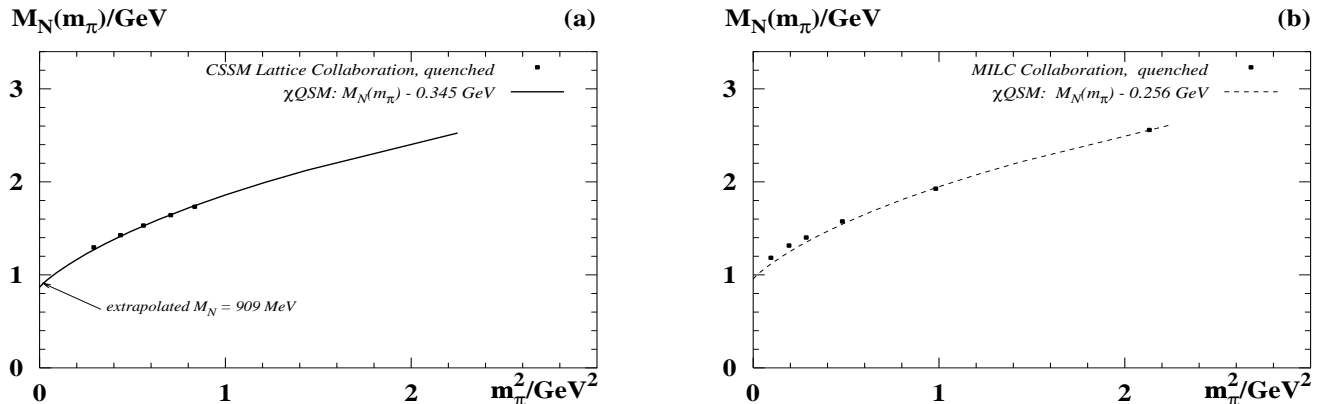


FIG. 3:  $M_N(m_\pi)$  vs.  $m_\pi^2$  from the chiral quark-soliton model vs. lattice data on  $M_N(m_\pi)$  obtained in the quenched approximation by 3a the CSSM Lattice Collaboration [10] and 3b the MILC Collaboration [9].

fects can be assumed to be small. Also, in this work we consider data obtained from lattices with spacings  $a \leq 0.13$  fm and assume discretization effects to be negligible. Such effects are difficult to control systematically [40].

In Fig. 2b the  $\chi$ QSM result for  $M_N(m_\pi)$  is compared to lattice data by the JLQCD Collaboration from Ref. [5], where dynamical simulations with two flavours were performed on a  $20^3 \times 48$  lattice using the plaquette gauge action and the non-perturbatively  $\mathcal{O}(a)$  improved Wilson quark action at  $\beta = 5.20$  with lattice spacings  $0.10 \text{ fm} \leq a \leq 0.13 \text{ fm}$ . The physical size of the lattice was  $1.96 \text{ fm} \leq L \leq 2.53 \text{ fm}$  and the range  $500 \text{ MeV} \leq m_\pi \leq 1 \text{ GeV}$  was covered corresponding to  $m_\pi L > 5$ . The best fit yields  $C = 341 \text{ MeV}$  with a  $\chi_{\text{dof}}^2 = 0.3$  and is shown in Fig. 2b.

In Figs. 2c and d we compare  $M_N(m_\pi)$  from the model to lattice results by the CP-PACS Collaboration [4], which were obtained on  $24^3 \times 48$  lattices from a renormalization-group improved gauge action and a mean field improved clover quark action at  $\beta = 2.1$  (and  $\beta = 2.2$ ) with dynamical  $u$ - and  $d$ -quarks and quenched  $s$ -quarks. For hadrons with no valence  $s$ -quarks this practically means a full two-flavour simulation. The physical lattice spacings and sizes were  $a = 0.09 \text{ fm}$  to  $0.13 \text{ fm}$  and  $L = 2.22 \text{ fm}$  to  $3.12 \text{ fm}$  with pion masses in the range  $500 \text{ MeV} \leq m_\pi \leq 1 \text{ GeV}$ , such that  $m_\pi L \gtrsim 7$ . We observe that  $M_N(m_\pi)$  from the  $\chi$ QSM with a subtraction constant  $C = 331 \text{ MeV}$  with  $\chi_{\text{dof}}^2 = 2.2$  (and  $C = 338 \text{ MeV}$  with  $\chi_{\text{dof}}^2 = 0.4$ ) describes well the lattice data of Ref. [4], see Fig. 2c (and Fig. 2d).

Next we confront the model results for  $M_N(m_\pi)$  to lattice data from dynamical two-flavour simulations with domain wall fermions by the RBC Collaboration [8], which have the virtue of preserving chiral invariance. In Ref. [8] a renormalization group improved (“doubly blocked Wilson”) gauge action with  $\beta = 0.80$  was used on a  $16^3 \times 32$  lattice with the physical spacing of  $0.12 \text{ fm}$  and a lattice size about  $2 \text{ fm}$ . The range of pion masses was  $m_\pi = 470 \text{ MeV}$  to  $650 \text{ MeV}$ . A best fit yields for the constant  $C = 306 \text{ MeV}$  with a  $\chi_{\text{dof}}^2 = 0.02$ , and provides a very good description of the data, see Fig. 2e.

In Fig. 2f we confront  $M_N(m_\pi)$  from the  $\chi$ QSM with lattice data by the MILC Collaboration [9] obtained from simulations with three dynamical quarks using a one-loop Symanzik improved gauge action and an improved Kogut-Susskind quark action. The physical lattice size was tuned to  $L = 2.6 \text{ fm}$  with a lattice spacing of  $0.13 \text{ fm}$  and the range of pion masses  $340 \text{ MeV} \leq m_\pi \leq 2.2 \text{ GeV}$  was covered. The best fit yields  $C = 256 \text{ MeV}$  for the subtraction constant (with  $\chi_{\text{dof}}^2 = 1.2$ ).

One could worry whether the SU(2) model results can be compared to three-flavour lattice simulations, though in [9] for the nucleon mass no significant differences were noticed between two- and three-flavour runs. However, as noted in Sec. II, the nucleon mass is the same in the SU(2) and SU(3) versions of the  $\chi$ QSM if  $m_u = m_d = m_s$ , which is the case for the lattice data [9] for  $m_\pi > 700 \text{ MeV}$ . Restricting the fitting procedure to this range of  $m_\pi$  (the last three points in Fig. 2f) we obtain  $C = 260 \text{ MeV}$  (with a  $\chi_{\text{dof}}^2 = 1.9$ ). This fit is shown in Fig. 2f. Note that it is practically indistinguishable, c.f. footnote 1, from the fit where the whole  $m_\pi$ -range (i.e. also data with  $m_u = m_d < m_s$ ) was used, and equally

well describes the region of lower  $m_\pi$ . In any case we observe a good agreement with the lattice data [9] up to  $m_\pi = 1.5 \text{ GeV}$ .

It is instructive to compare the model results also to lattice data obtained from simulations performed in the *quenched* approximation, e.g., by the CSSM Lattice Collaboration [10], where a mean-field improved gauge action and a fat-link clover fermion (“FLIC”) action was used on a  $16^3 \times 32$  lattice with a lattice spacing of  $a = 0.125 \text{ fm}$ . The calculation covers the range  $540 \text{ MeV} \leq m_\pi \leq 920 \text{ MeV}$ . A best fit to the quenched data gives  $C = 345 \text{ MeV}$  (with a  $\chi_{\text{dof}}^2 = 1.3$ ) which yields a good agreement with the lattice data, see Fig. 3a.

For the quenched data by the MILC Collaboration [9], however, we observe that a fit would work much worse. In this case we refrain from fitting and show instead in Fig. 3b the fit to the full MILC data from Fig. 2f, which nicely illustrates how results from full and quenched calculations differ. Interestingly, at large  $m_\pi^2$  the full and quenched data of Ref. [9] agree well with each other. In fact, it is not surprising that differences between full and quenched simulations become less pronounced with increasing  $m_\pi^2$ , i.e. with increasing fermion masses.

From the  $[M_N(m_\pi) - C]$  at  $m_\pi = 140 \text{ MeV}$  with the constant  $C$  fitted to the respective data, we obtain the physical value of the nucleon mass – extrapolated by means of the  $\chi$ QSM as a guideline. The extrapolated values are indicated by arrows in Figs. 2a-f and 3a, and are summarized in the Table II.

It is worthwhile stressing that the extrapolated values in Table II agree within an accuracy of  $\pm 5\%$  with the physical mass of the nucleon. The theoretical accuracy of this extrapolation is discussed in the next section.

TABLE II: *The value of the physical nucleon mass  $M_N$  (in MeV) extrapolated from lattice calculations [4–10] using the  $\chi$ QSM as guideline, see text. For convenience the physical lattice sizes and spacings (in fm) and the covered range of  $m_\pi$  (in MeV) are included, and the  $\chi_{\text{dof}}^2$  of the fit. The uncertainty of the fits due to the statistical error of lattice data is of the order of few MeV and thus practically negligible, see the remark in footnote 1.*

Collaboration	lattice size	spacing	$m_\pi$ -range	$M_N$	$\chi_{\text{dof}}^2$
UKQCD [6, 7]	2.0-2.2	0.09-0.12	550-940	925	0.7
JLQCD [5]	2.0-2.5	0.10-0.13	540-960	913	0.3
CP-PACS [4] ( $\beta = 2.1$ )	2.7-3.1	0.11-0.13	520-960	922	2.2
CP-PACS [4] ( $\beta = 2.2$ )	2.2-2.4	0.09-0.10	590-970	915	0.4
RBC [8]	1.9-2.0	0.12	470-650	947	0.02
MILC [9] (all data)	2.6	0.13	350-1500	998	1.2
MILC [9] (only $m_u, d = m_s$ )	2.6	0.13	720-1500	993	1.9
CSSM [10] (quenched)	2.0	0.125	540-920	909	1.3

#### IV. COMPARISON TO $\chi$ PT AND FRR

It is instructive to compare our  $\chi$ QSM-based extrapolation of lattice data to other approaches based on  $\chi$ PT [7, 13–15] and the finite range regulator (FRR) method of Ref. [21]. The comparison will shed some light on the question, how a model based on the large- $N_c$  expan-

sion can provide a reliable description of lattice data on  $M_N(m_\pi)$  observed in Sec. III.

First we address the question of the range of reliability of the method. It was argued that  $\chi$ PT to  $\mathcal{O}(p^4)$  provides a reliable expansion for  $M_N(m_\pi)$  up to  $m_\pi^2 < 0.4 \text{ GeV}^2$  [13–15] ( $p$  is to be identified with the generic small expansion parameter in  $\chi$ PT, e.g., in our context pion mass). A more conservative bound  $m_\pi^2 < 0.1 \text{ GeV}^2$  was given in [16]. The FRR method was argued to correspond to a *partial* resummation of the chiral expansion, and to be valid up to  $m_\pi^2 < 1 \text{ GeV}^2$  [21].

What might be the range of reliability of the  $\chi$ QSM? Recall that the  $\chi$ QSM expression for the nucleon mass (as well as for any other quantity) may be considered as a resummed infinite series in derivatives of the chiral field  $U = \exp(i\tau^a \pi^a)$ , c.f. Eq. (11), whereby it is understood that each chiral order is evaluated in the large- $N_c$  limit. (Note that these limits do not commute, see Sect. II B.) Thus, one may argue that the  $\chi$ QSM corresponds to a chiral expansion, which is *completely* resummed – to leading order of the large- $N_c$  expansion. If one were happy with this approximation, then  $\chi$ QSM results could be considered reliable for all  $m_\pi$  including the heavy quark limit, see the discussion in Sec. II C.

What might be the effects due to  $1/N_c$ -corrections? Let us consider the mass difference between the  $\Delta$ -resonance and the nucleon as a measure for such corrections. Note that this mass difference vanishes not only in the large- $N_c$  limit, see Eq. (16), but also in the heavy quark limit [32]. This is supported by lattice results [4, 9, 10], where always  $\Delta \equiv M_\Delta - M_N < m_\pi$  holds. (This means that on present day lattices the  $\Delta$ -resonance is safe from strong decays and thus a stable particle.) In the region  $m_\pi^2 > 0.32 \text{ GeV}^2$  one finds  $\Delta < \frac{1}{5}m_\pi$  [4, 9, 10]. Thus, practically for most of the present day lattice data the condition

$$\Delta \equiv M_\Delta - M_N \ll m_\pi \text{ for } m_\pi^2 > 0.32 \text{ GeV}^2 \quad (19)$$

is satisfied, such that the  $\Delta$ -nucleon mass difference can be neglected to a good approximation. This may be a reason for the good description of lattice data in the  $\chi$ QSM up to  $m_\pi^2 \leq 2.3 \text{ GeV}^2$  in Sec. III.

However, in the physical region  $\Delta = 290 \text{ MeV}$  is larger than  $m_\pi = 140 \text{ MeV}$ , and the leading order large- $N_c$  treatment of the nucleon mass inevitably introduces a systematic error. In fact, one could express the nucleon mass as a function  $F(x, y)$  of  $x = m_\pi$  and  $y = \Delta/m_\pi$  as

$$M_N(m_\pi, \Delta) = F\left(m_\pi, \frac{\Delta}{m_\pi}\right). \quad (20)$$

Then, using the  $\chi$ QSM as a guideline for the extrapolation of lattice data corresponds to approximating

$$M_N = F(m_\pi, 2.1) \approx F(m_\pi, 0) \text{ at } m_\pi = 140 \text{ MeV}. \quad (21)$$

It is difficult to quantify the systematic error associated with this approximation. A comparison to  $\chi$ PT and the FRR method may give us a rough idea about the size of the effect.

Let us next discuss in some detail how  $\chi$ PT can be used as a tool to extrapolate lattice data – in particular we shall focus on the analyses [7, 14]. In  $\chi$ PT up to  $\mathcal{O}(p^4)$  one has 4 free parameters in the chiral expansion of the nucleon mass. Hereby one faces the problem

that an expansion to higher order in  $\chi$ PT has a better convergence but introduces more free parameters. The free parameters can in principle be determined from a fit to lattice data. In practice, restricting oneself to the believed radius of convergence of  $\chi$ PT to  $\mathcal{O}(p^4)$ , namely  $m_\pi < 600 \text{ MeV}$ , the present lattice data do not allow to constrain more than 3 free parameters [14].

Thus, e.g., in the  $\mathcal{O}(p^4)$ -analyses of lattice data in Refs. [7, 14] the fact was used that some of the parameters appearing in the chiral expansion of  $M_N(m_\pi)$  are known with a certain precision from empirical studies of nucleon-nucleon or pion-nucleon low-energy scattering analyses. Moreover in [14] the physical value of the nucleon mass was included as a constraint to the fit. Fig. 4a shows the  $M_N(m_\pi)$  as obtained in  $\chi$ PT to  $\mathcal{O}(p^4)$  from 3-parameter-fits to the lattice data [4–7] satisfying  $a < 0.15 \text{ fm}$ ,  $m_\pi L > 5$  and respectively the constraint  $m_\pi < 800 \text{ MeV}$  in Ref. [7], and  $m_\pi < 600 \text{ MeV}$  in Ref. [14].

For comparison in Fig. 4a our  $\chi$ QSM-1-parameter-fit to the same data set is shown. Note that the two highest- $m_\pi$  data points (marked by empty circles in Fig. 4a) by the UKQCD Collaboration [6, 7] were obtained from somehow smaller lattices of the size  $L = 1.56 \text{ fm}$  and  $1.68 \text{ fm}$  and clearly do not follow the tendency of the  $M_N(m_\pi)$  from the  $\chi$ QSM. These points are therefore omitted from the fit shown in Fig. 4a. Including these points significantly worsens the  $\chi_{\text{dof}}^2$  of the fit, see Table III where the results are summarized.

TABLE III: The value of the physical nucleon mass  $M_N$  as extrapolated by means of  $\chi$ PT to  $\mathcal{O}(p^4)$  lattice data [4–7] subject to the constraints  $a < 0.15 \text{ fm}$ ,  $m_\pi L > 5$  and respectively  $m_\pi < 800 \text{ MeV}$  in Ref. [7], and  $m_\pi < 600 \text{ MeV}$  in Ref. [14]. For comparison the  $\chi$ QSM-fits to the same data set, and to the same data set subject to the additional condition  $L \geq 2 \text{ fm}$  are shown. The error of  $M_N$  due to the statistical uncertainty of the lattice data and the  $\chi_{\text{dof}}^2$  of the fit are shown. The systematic error of  $M_N$  due to the extrapolation method, as well as lattice discretization or finite size effects, is merely indicated. (See the remark in footnote 1 concerning the small error of the  $\chi$ QSM-fit due to the statistical uncertainty of lattice data.)

Method	$M_N$ in MeV	$\chi_{\text{dof}}^2$
$\chi$ PT to $\mathcal{O}(p^4)$ , “Fit I” in Ref. [7]	$948 \pm 60 \pm \text{syst}$	1.7
$\chi$ PT to $\mathcal{O}(p^4)$ , “Fit II” in Ref. [14]	938 (fixed)	–
$\chi$ QSM (only $L \gtrsim 2 \text{ fm}$ )	$927 \pm 4 \pm \text{syst}$	0.5
$\chi$ QSM (all data points)	$931 \pm 4 \pm \text{syst}$	2.3

Since the  $\chi$ QSM-description of the lattice data remains effectively valid also at significantly larger  $m_\pi$ , see Sec. III, we conclude that, quoting Ref. [14], “*the surprisingly good (and not yet understood) agreement with lattice data [above  $m_\pi > 600 \text{ MeV}$ ] even up to  $m_\pi \approx 750 \text{ MeV}$ ” could be a somehow accidental consequence of comparing  $\chi$ PT to  $\mathcal{O}(p^4)$  at the edge (if not above) its range of applicability to lattice data where finite size effects start to play a role.*

In fact, up to  $m_\pi \lesssim (500 - 550) \text{ MeV}$  the  $\chi$ PT to  $\mathcal{O}(p^4)$  [7, 14] and the  $\chi$ QSM describe  $M_N(m_\pi)$  in good qualitative agreement, see Fig. 4a. Beyond this point, however, the nucleon mass as function of  $m_\pi^2$  from  $\chi$ PT changes the

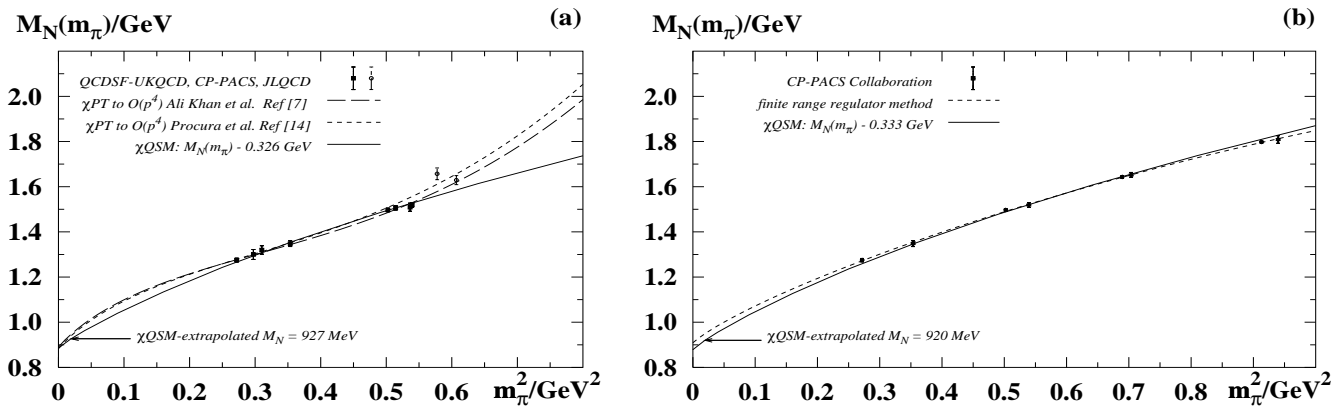


FIG. 4: Comparison of the results for  $M_N(m_\pi)$  as obtained from fitting lattice data selected from Refs. [4–7] in (a)  $\chi$ PT to  $\mathcal{O}(p^4)$  (“Fit I” from [7] and “Fit II” in [14]) and (b) the finite range regulator approach (with a dipole regulator) [21], and the respective 1-parameter  $\chi$ QSM-fits.

curvature. This contrasts the  $\chi$ QSM-result exhibiting negative curvature up to the highest considered  $m_\pi^2$ . This observation indicates that the range of reliability of  $\chi$ PT to  $\mathcal{O}(p^4)$  could be  $m_\pi \lesssim 500$  MeV (which, in fact, is not far from the generally assumed bound  $m_\pi < 600$  MeV).

With the above considerations in mind, we conclude that the  $\chi$ QSM describes lattice data [4–7] constrained by  $a < 0.15$  fm,  $m_\pi L > 5$  and  $L \geq 2$  fm very well, see Fig. 4a. In the range below  $m_\pi \lesssim 500$  MeV we observe a good qualitative and quantitative agreement of the  $\chi$ QSM with  $\chi$ PT to  $\mathcal{O}(p^4)$  [7, 14]. In this range the curves for  $M_N(m_\pi)$  from the two approaches agree with each other to within an accuracy of 50 MeV and better, see Fig. 4a. This number may give us a flavour of the magnitude of the systematic error of the  $\chi$ QSM-extrapolation of lattice data, though  $\chi$ PT to  $\mathcal{O}(p^4)$  may also have such an intrinsic uncertainty, as indicated in Table III, due to unestimated contributions from  $\mathcal{O}(p^5)$ .

Next we consider the finite range regulator (FRR) method of Ref. [21] where 5 free parameters appear, which can well be constrained by lattice data thanks to the larger range of applicability of the approach, namely up to  $m_\pi^2 = 1$  GeV<sup>2</sup>. In Ref. [21] different shapes of regulators were exploited and shown to yield practically the same results. Fig. 4b shows the 5-parameter fit (using the dipole-type regulator) to the CP-PACS lattice data sets with  $\beta = 2.1$  and  $2.2$  from Ref. [4]. In the  $\chi$ QSM-approach with one free parameter only, we were able to fit both data sets separately, see Figs. 2c and d. For sake of comparison we include the combined  $\chi$ QSM-fit in Fig. 4b and summarize the results in Table IV.

As demonstrated in Fig. 4b and Table IV the results for  $M_N(m_\pi)$  from the FRR approach and the  $\chi$ QSM describe the CP-PACS data [4] equally well. Having a closer look on the region  $m_\pi^2 < 0.3$  GeV<sup>2</sup> we see that  $M_N(m_\pi)$  from the  $\chi$ QSM starts to deviate more and more strongly from the fit of the FRR-approach with decreasing  $m_\pi^2$ , though the curves remain very similar. The reason for the discrepancy (which apparently was of no relevance for  $m_\pi^2 > 0.3$  GeV<sup>2</sup>, see Fig. 4b) should be attributed to the fact, that  $M_\Delta - M_N$  is kept finite in the FRR approach, but neglected in the  $\chi$ QSM.

At the physical point the difference between the values of  $M_N$  extrapolated by means of the FRR method and the  $\chi$ QSM is about 40 MeV, which again may give us a

TABLE IV: The value of the physical nucleon mass  $M_N$  as extrapolated from CP-PACS lattice data [4] obtained from lattices of the sizes  $L = (2.2 - 3.1)$  fm with lattice spacings  $a = (0.09 - 0.13)$  fm covering the range  $520 \text{ MeV} \leq m_\pi \leq 970 \text{ MeV}$ . As guidelines for the extrapolation were used the finite range regulator approach [21] and the  $\chi$ QSM. See also the remarks in the caption to Table III.

Method	$M_N$ in MeV	$\chi^2_{\text{dof}}$
finite range (“dipole”) regulator [21]	$959 \pm 116 \pm \text{syst}$	0.4
$\chi$ QSM	$920 \pm 3 \pm \text{syst}$	1.2

rough idea on the theoretical uncertainty due to neglecting the  $\Delta$ -nucleon mass difference. Note that for this rough estimate we use the central value of the extrapolated  $M_N$  from the FRR approach, see Table IV, which has a substantially larger statistical uncertainty arising from fitting 5 parameters to the lattice data. In this respect the 1-parameter  $\chi$ QSM-fit is far more precise.

The comparison of the  $\chi$ QSM-based fits and those obtained using  $\chi$ PT [7, 14] and the FRR approach [21] leads us to the following conclusion. The systematic uncertainty of  $M_N$  due to neglecting the finite  $\Delta$ -nucleon mass-splitting in the  $\chi$ QSM is effectively about (40 – 50) MeV with the tendency to underestimate the nucleon mass. Recall that we do not consider isospin breaking effects or electromagnetic corrections, see footnote 1, which are of  $\mathcal{O}(10 \text{ MeV})$ . Thus, we have to assign a systematic error to the  $\chi$ QSM-fits of about

$$(\delta M_N)_{\text{syst}} \simeq 60 \text{ MeV}. \quad (22)$$

Noteworthy, a similar result – concerning both the sign and the order of magnitude – follows from a crude estimate within the model itself, see App. C.

We stress that it is not possible to quantify the uncertainty of the  $\chi$ QSM-extrapolation of lattice data more quantitatively than that. Taking into account the systematic error (22) we observe that the extrapolated values in Tables II, III and IV are all consistent with the physical mass of the nucleon.

## V. CONCLUSIONS

The implicit dependence of the nucleon mass  $M_N$  on the pion mass  $m_\pi$  was studied in the large- $N_c$  limit in the framework of the chiral quark soliton model. The  $M_N(m_\pi)$  in the model exhibits the correct behaviour in the chiral limit including correct (in the large- $N_c$ -limit) leading non-analytic terms [31]. As was shown here, the model describes correctly also the heavy quark limit.

These properties make the  $\chi$ QSM an appealing ground for the chiral extrapolation of lattice data. In fact, we have shown that the  $\chi$ QSM well describes lattice data from full simulations [3–9] over the wide range of pion masses  $0.1 \text{ GeV}^2 < m_\pi^2 < 2.5 \text{ GeV}^2$ , provided one takes into account the generic overestimate of the nucleon mass in the soliton approach [37]. This is done by introducing an  $m_\pi$ -independent subtraction constant, i.e. one single parameter to be fitted to the respective lattice data set.

The values for the nucleon mass extrapolated from the lattice results [3–10] on the basis of results from the  $\chi$ QSM agree with the physical nucleon mass within 5%, and are in good agreement with extrapolations based on other approaches [7, 14, 21].

The main limitation for using the  $\chi$ QSM as a quantitative tool to extrapolate lattice data is due to the non-commutativity of the chiral limit and the large- $N_c$  limit. In leading order of the large- $N_c$  limit the nucleon and the  $\Delta$ -resonance are mass degenerated, i.e. in our approach the  $\Delta$ -nucleon mass-splitting  $\Delta = M_\Delta - M_N$  is neglected.

This is not an obstacle for the description of presently available lattice data, because  $\Delta \rightarrow 0$  not only in the large- $N_c$  limit but also in the heavy-quark limit, i.e. the larger  $m_\pi$  the smaller  $\Delta$ . For most of the present day lattice data the inequality  $m_\pi^2 \gg \Delta^2$  holds. In this region the neglect of a finite  $\Delta$ -nucleon mass-splitting appears a reasonable approximation. When extrapolating lattice data to the physical point, however, the neglect of a finite  $\Delta$ -nucleon mass-splitting introduces a systematic error. We roughly estimate this error to be of  $\mathcal{O}(60 \text{ MeV})$  at the physical value of the pion mass.

However, what is most interesting for lattice practitioners are extrapolations with well *controlled* systematic uncertainties and precise error estimates, which could help to better understand intrinsic uncertainties of lattice calculations such as discretization errors or finite size effects. Nevertheless the  $\chi$ QSM may act as a bridge between lattice QCD and chiral extrapolation – providing valuable insights in the presently narrow “overlap region” where first lattice data are already available and where chiral perturbation theory is still reliable. Further studies in this direction are in progress.

### Acknowledgments

We thank Pavel Pobylitsa, Maxim Polyakov, Gerit Schierholz, Wolfram Schroers and Tony Thomas for fruitful discussions and valuable comments. This research is part of the EU integrated infrastructure initiative hadron physics project under contract number RII3-CT-2004-506078, and partially supported by the Graduierten-Kolleg Bochum-Dortmund and Verbundforschung of BMBF. A. S. acknowledges support from GRICES and DAAD.

## APPENDIX A: PROPER-TIME REGULARIZATION

The proper-time regularized versions of the integrals  $I_1$  and  $I_2$  appearing in Eqs. (2, 4) are given by

$$I_1(m) = \int_{\Lambda_{\text{cut}}^{-2}}^{\infty} \frac{du}{u^2} \frac{\exp(-uM'^2)}{(4\pi)^2}, \quad (\text{A1})$$

$$I_2(m) = \int_{\Lambda_{\text{cut}}^{-2}}^{\infty} \frac{du}{2u} \frac{\exp(-uM'^2)}{(4\pi)^2} \int_0^1 d\beta \exp(u\beta(1-\beta)m_\pi^2)$$

where the  $m$ -dependence is hidden in  $M' \equiv M + m$ . For a given  $m_\pi$  and  $f_\pi = 93 \text{ MeV}$  fixed and due to Eqs. (4, 5) both the current quark mass and the cutoff are (implicit) functions of  $m_\pi$ , i.e.  $m = m(m_\pi)$  and  $\Lambda_{\text{cut}} = \Lambda_{\text{cut}}(m_\pi)$ ; some selected values are shown in Table I.

The expression for the soliton energy (9) in the proper-time regularization is given by

$$E_{\text{sol}} = N_c \left[ E_{\text{lev}} + \sum_n (R(E_n) - R(E_{n_0})) \right];$$

$$R(\omega) = \frac{1}{4\sqrt{\pi}} \int_{\Lambda_{\text{cut}}^{-2}}^{\infty} \frac{du}{u^{3/2}} \exp(-u\omega^2). \quad (\text{A2})$$

## APPENDIX B: THE PION-NUCLEON SIGMA-TERM $\sigma_{\pi N}$

The pion-nucleon sigma-term is an important quantity to learn about chiral symmetry breaking effects in the nucleon. The Feynman-Hellmann theorem [41] relates  $\sigma_{\pi N}$  to the slope of  $M_N(m)$  (with  $m = m_q = m_u = m_d$  neglecting isospin breaking effects) as follows

$$\sigma_{\pi N} \equiv m \frac{\partial M_N(m)}{\partial m} = m_\pi^2 \frac{\partial M_N(m_\pi)}{\partial m_\pi^2} \quad (\text{B1})$$

where the second equality holds, strictly speaking, only for small  $m_\pi$ . Apart from (B1) one also can evaluate in the model directly the actual definition of  $\sigma_{\pi N}$  as double commutator of the strong interaction Hamiltonian with two axial isovector charges [42, 43], or exploit a sum rule for the twist-3 distribution function  $e(x)$  [44]. All three methods yield the same result in the  $\chi$ QSM [31].

In the  $\chi$ QSM the pion-nucleon sigma-term is quadratically UV-divergent, and as such particularly sensitive to details of regularization. In Ref. [31] a way was found to compute  $\sigma_{\pi N}$  in a regularization scheme independent way with the result  $\sigma_{\pi N} \approx 68 \text{ MeV}$ . The price to pay for the regularization scheme independence was the use of an *approximation* expected to work within an accuracy of  $\mathcal{O}(30\%)$  and well-justified by notions from the instanton vacuum model. On the basis of our results for  $M_N(m_\pi)$  we are now in a position to check the accuracy of this approximation in practice. For that we note that the Feynman-Hellmann relation (B1) allows to determine  $M_N(m_\pi)$  from  $\sigma_{\pi N}(m_\pi)$  up to an integration constant.

From the approximate (but regularization scheme independent) result for  $\sigma_{\pi N}(m_\pi)$  from Ref. [31] one obtains for  $M_N(m_\pi)$  the result shown as dashed line in Fig. 1,

where for convenience the integration constant is chosen such that both curves coincide at a central value of  $m_\pi = 1$  GeV in the plot. We observe a good agreement of the exact result and the approximation of Ref. [31], see Fig. 1. In the proper-time regularization we obtain by means of Eq. (B1) the result  $\sigma_{\pi N} = 40$  MeV, which agrees well with other calculations in the model [27, 42, 43] performed in this regularization scheme, as well as with the regularization scheme-independent result of [31] to within the expected accuracy of  $\mathcal{O}(30\%)$ .

Thus, our results confirm that the instanton model motivated approximation advocated in [31] works well. Note, however, that here we went far beyond the study of Ref. [31]. In this work we practically demonstrated that stable soliton solutions *do exist* also for large values of the pion mass, while in Ref. [31] this was *presumed*.

The regularization scheme independent result of Ref. [31] is in good agreement with recent extractions indicating  $\sigma_{\pi N} = (60 - 70)$  MeV [45], which is substantially more sizeable than the value obtained from earlier analyses [46].

In this context it is worthwhile mentioning that the spectrum of exotic ("pentaquark") baryons which were predicted in the framework of the  $\chi$ QSM [47] and for which recently possible observations were reported – see [48] for recent overviews – could provide an independent mean to access information on the pion-nucleon sigma-term [49]. The presently available data on the exotic baryons favour a large value for  $\sigma_{\pi N}$  as found in [45].

### APPENDIX C: SYSTEMATIC UNCERTAINTY OF THE ROTATING SOLITON APPROACH

The neglect of  $\Delta = M_\Delta - M_N$  in the leading order of the large- $N_c$  limit introduces a systematic uncertainty

which is difficult to quantify. Here we roughly estimate this uncertainty on the basis of the soliton approach.

In this approach the nucleon and the  $\Delta$ -resonance are just different rotational excitations of the same classic object, the soliton. A non-zero mass difference between the nucleon and the  $\Delta$ -resonance arises due to considering a particular class of ("rotational")  $1/N_c$ -corrections [22, 23]. The mass of an  $SU(2)$ -baryon  $M_B$  ( $B = N$  or  $\Delta$  in the real world with  $N_c = 3$  colours) with spin  $S_B$  is given by

$$M_B = E_{\text{sol}} + M_2 + S_B(S_B + 1) \frac{\Delta}{3} + \dots \quad (\text{C1})$$

with  $E_{\text{sol}}$  as defined in Eq. (9),  $M_2$  denoting as in Eq. (12) the  $\mathcal{O}(N_c^0)$  correction to the baryon mass which is the same for the nucleon and the  $\Delta$ -resonance, and the dots representing higher order  $1/N_c$ -corrections.

Then we obtain as a first correction to  $M_N$  in Eq. (21)

$$M_N(m_\pi, \Delta) = M_N(m_\pi, 0) + \frac{\Delta(m_\pi)}{4} + \dots \quad (\text{C2})$$

Focusing on the linear order correction in  $\Delta$  and neglecting higher orders, we see that by neglecting  $\Delta$  one underestimates the nucleon mass by about 70 MeV at the physical value of the pion mass. This is in good agreement with the systematic uncertainty estimated in Eq. (22).

- 
- [1] K. G. Wilson, Phys. Rev. D **10** (1974) 2445.  
[2] M. Creutz, "Quarks, Gluons And Lattices", (Cambridge University Press, Cambridge, 1983).  
C. Rebbi, "Lattice Gauge Theories and Monte Carlo Simulations", (World Scientific, Singapore, 1983).  
[3] S. Aoki *et al.* [CP-PACS Collaboration], Phys. Rev. D **60** (1999) 114508 [arXiv:hep-lat/9902018], and Phys. Rev. D **67** (2003) 034503 [arXiv:hep-lat/0206009].  
[4] A. Ali Khan *et al.* [CP-PACS Collaboration], Phys. Rev. D **65** (2002) 054505 [Erratum-ibid. D **67** (2003) 059901].  
[5] S. Aoki *et al.* [JLQCD Collaboration], Phys. Rev. D **68** (2003) 054502 [arXiv:hep-lat/0212039].  
[6] C. R. Allton *et al.* [UKQCD Collaboration], Phys. Rev. D **65** (2002) 054502 [arXiv:hep-lat/0107021].  
[7] A. Ali Khan *et al.* [QCDSF-UKQCD Collaboration], Nucl. Phys. B **689** (2004) 175 [arXiv:hep-lat/0312030].  
[8] Y. Aoki *et al.*, arXiv:hep-lat/0411006.  
[9] C. W. Bernard *et al.* [MILC Collaboration], Phys. Rev. D **64** (2001) 054506 [arXiv:hep-lat/0104002].  
[10] J. M. Zanotti *et al.* [CSSM Lattice Collaboration], Phys. Rev. D **65** (2002) 074507 [arXiv:hep-lat/0110216].  
[11] J. Gasser, Annals Phys. **136**, 62 (1981).  
[12] J. Gasser and H. Leutwyler, Annals Phys. **158** (1984) 142.  
[13] V. Bernard, T. R. Hemmert and U. G. Meissner, Nucl. Phys. A **732** (2004) 149 [arXiv:hep-ph/0307115].  
[14] M. Procura, T. R. Hemmert and W. Weise, Phys. Rev. D **69** (2004) 034505 [arXiv:hep-lat/0309020].  
[15] M. Frink and U. G. Meissner, JHEP **0407** (2004) 028 [arXiv:hep-lat/0404018]. M. Frink, U. G. Meissner and I. Scheller, arXiv:hep-lat/0501024.  
V. Bernard, T. R. Hemmert and U. G. Meissner, arXiv:hep-lat/0503022.  
[16] S. R. Beane, Nucl. Phys. B **695** (2004) 192 [arXiv:hep-lat/0403030].  
[17] D. B. Leinweber, D. H. Lu and A. W. Thomas, Phys. Rev. D **60** (1999) 034014 [arXiv:hep-lat/9810005].  
[18] D. B. Leinweber, A. W. Thomas, K. Tsushima and S. V. Wright, Phys. Rev. D **61** (2000) 074502 [arXiv:hep-lat/9906027].  
[19] D. B. Leinweber, A. W. Thomas and S. V. Wright, Phys. Lett. B **482** (2000) 109 [arXiv:hep-lat/0001007].  
[20] R. D. Young, D. B. Leinweber, A. W. Thomas and S. V. Wright, Phys. Rev. D **66** (2002) 094507 [arXiv:hep-lat/0205017].  
[21] D. B. Leinweber, A. W. Thomas and R. D. Young, Phys. Rev. Lett. **92** (2004) 242002 [arXiv:hep-lat/0302020].  
[22] D. I. Diakonov and V. Y. Petrov, JETP Lett. **43** (1986) 75 [Pisma Zh. Eksp. Teor. Fiz. **43** (1986) 57].  
[23] D. I. Diakonov, V. Y. Petrov and P. V. Pobylitsa, Nucl. Phys. B **306**, 809 (1988).  
[24] D. I. Diakonov and V. Y. Petrov, Nucl. Phys. B **245**, 259 (1984).  
[25] D. I. Diakonov and V. Y. Petrov, Nucl. Phys. B **272**, 457

- (1986).
- [26] For reviews see: D. I. Diakonov and V. Y. Petrov, in *At the frontier of particle physics*, ed. M. Shifman (World Scientific, Singapore, 2001), vol. 1, p. 359-415 [arXiv:hep-ph/0009006]; D. Diakonov, *Prog. Part. Nucl. Phys.* **51** (2003) 173 [arXiv:hep-ph/0212026]; and arXiv:hep-ph/0406043.
- [27] D. I. Diakonov, V. Y. Petrov and M. Praszalowicz, *Nucl. Phys. B* **323** (1989) 53.
- [28] C. V. Christov *et al.*, *Prog. Part. Nucl. Phys.* **37**, 91 (1996).
- [29] D. I. Diakonov *et al.*, *Nucl. Phys. B* **480** (1996) 341 and *Phys. Rev. D* **56** (1997) 4069.  
K. Goeke, P. V. Pobylitsa, M. V. Polyakov, P. Schweitzer and D. Urbano, *Acta Phys. Polon. B* **32** (2001) 1201.  
P. Schweitzer, D. Urbano, M. V. Polyakov, C. Weiss, P. V. Pobylitsa and K. Goeke, *Phys. Rev. D* **64**, 034013 (2001).
- [30] V. Y. Petrov, P. V. Pobylitsa, M. V. Polyakov, I. Börnig, K. Goeke and C. Weiss, *Phys. Rev. D* **57** (1998) 4325.  
M. Penttinen, M. V. Polyakov and K. Goeke, *Phys. Rev. D* **62** (2000) 014024.  
P. Schweitzer *et al.*, *Phys. Rev. D* **66** (2002) 114004 and **67** (2003) 114022; *Nucl. Phys. A* **711** 207 (2002).  
J. Ossmann, M. V. Polyakov, P. Schweitzer, D. Urbano and K. Goeke, *Phys. Rev. D* **71**, 034011 (2005) [arXiv:hep-ph/0411172].
- [31] P. Schweitzer, *Phys. Rev. D* **69** (2004) 034003 [arXiv:hep-ph/0307336].
- [32] R. F. Dashen, E. Jenkins and A. V. Manohar, *Phys. Rev. D* **49**, 4713 (1994) [Erratum-ibid. *D* **51**, 2489 (1995)].
- [33] T. D. Cohen and W. Broniowski, *Phys. Lett. B* **292**, 5 (1992) [arXiv:hep-ph/9208253].
- [34] D. I. Diakonov and M. I. Eides, *JETP Lett.* **38**, 433 (1983) [*Pisma Zh. Eksp. Teor. Fiz.* **38** (1983) 358].
- [35] A. Dhar, R. Shankar and S. R. Wadia, *Phys. Rev. D* **31** (1985) 3256.
- [36] E. Witten, *Nucl. Phys. B* **223**, 433 (1983).
- [37] P. V. Pobylitsa, E. Ruiz Arriola, T. Meissner, F. Grummer, K. Goeke and W. Broniowski, *J. Phys. G* **18** (1992) 1455.
- [38] R. Sommer, *Nucl. Phys. B* **411** (1994) 839 [arXiv:hep-lat/9310022].
- [39] R. Sommer *et al.* [ALPHA Collaboration], *Nucl. Phys. Proc. Suppl.* **129** (2004) 405 [arXiv:hep-lat/0309171].
- [40] O. Bär, *Nucl. Phys. Proc. Suppl.* **140** (2005) 106 [arXiv:hep-lat/0409123].
- [41] H. Hellmann, “Einführung in die Quantenchemie” [Leipzig, Deuticke Verlag, 1937].  
R. P. Feynman, *Phys. Rev.* **56**, 340 (1939).
- [42] M. Wakamatsu, *Phys. Rev. D* **46**, 3762 (1992).
- [43] H. C. Kim, A. Blotz, C. Schneider and K. Goeke, *Nucl. Phys. A* **596**, 415 (1996).
- [44] P. Schweitzer, *Phys. Rev. D* **67** (2003) 114010 [arXiv:hep-ph/0303011]. For an overview on  $\epsilon(x)$  see: A. V. Efremov and P. Schweitzer, *JHEP* **0308** (2003) 006 [arXiv:hep-ph/0212044].
- [45] W. B. Kaufmann and G. E. Hite, *Phys. Rev. C* **60**, 055204 (1999). M. G. Olsson, *Phys. Lett. B* **482**, 50 (2000).  
M. M. Pavan, I. I. Strakovsky, R. L. Workman and R. A. Arndt,  *$\pi$ N Newsletter* **16**, 110-115 (2002) [arXiv:hep-ph/0111066].  
M. G. Olsson and W. B. Kaufmann, *PiN Newslett.* **16**, 382 (2002).
- [46] R. Koch, *Z. Phys. C* **15**, 161 (1982).  
J. Gasser, H. Leutwyler and M. E. Sainio, *Phys. Lett. B* **253** 252, and 260 (1991).
- [47] D. I. Diakonov, V. Y. Petrov and M. V. Polyakov, *Z. Phys. A* **359** (1997) 305 [arXiv:hep-ph/9703373].
- [48] K. Hicks, arXiv:hep-ex/0412048.  
T. Nakano, *Nucl. Phys. A* **738** (2004) 182.
- [49] P. Schweitzer, *Eur. Phys. J. A* **22** (2004) 89 [arXiv:hep-ph/0312376].